



Research article

Remote examination of the seasonal succession of phytoplankton assemblages from time-varying trends



Botian Zhou^a, Mingsheng Shang^a, Sheng Zhang^b, Li Feng^b, Xiangnan Liu^c, Ling Wu^c, Lei Feng^a, Kun Shan^{a,*}

^a Chongqing Key Laboratory of Big Data and Intelligent Computing, Chongqing Institute of Green and Intelligent Technology, Chinese Academy of Sciences, Chongqing, 400714, China

^b Chongqing Collaborative Innovation Center of Big Data Application in Eco-Environmental Remote Sensing, Chongqing Academy of Environmental Science, Chongqing, 401147, China

^c School of Information Engineering, China University of Geosciences, Beijing, 100083, China

ARTICLE INFO

Keywords:

Phytoplankton succession
Temporal pattern
Time series analysis
Huan Jing 1 charge-coupled device image
Cyano-chlorophyta index
Three gorges reservoir

ABSTRACT

The seasonal succession of phytoplankton assemblages is important to ascertain the dynamics of an aquatic ecosystem structure, whereas its occurrence in response to hydrodynamic alterations is not clearly understood. In view of the characteristics of annual water level variation formed by the Three Gorges Dam Project (TGDP), our understanding about how these changes affect phytoplankton structure and dynamics is still very limited due to the shortage of long-term observation data. In this study, we used Huan Jing 1 charge-coupled device images over the past decade to examine the phytoplankton succession dates between cyanobacterial and green algal blooms in the backwater area of the Three Gorges Reservoir (TGR). The results indicated continuous wavelet transform-based peak analysis is an efficiency tool that can illustrate the temporal pattern of phytoplankton succession using satellite-derived chlorophyll *a* and Cyano-Chlorophyta index thresholds. Water level, air temperature, pH and total nitrogen/total phosphorus ratio were four important factors affecting the decline and rise phase of cyanobacterial blooms in the TGR from 2008 to 2018. Given that the upstream dam operation is likely to alter ecological and environmental conditions in the backwater area, this mechanism, so-called “water-level linkage”, could alleviate the persistent period of cyanobacterial and green algal blooms. Remote sensing together with time series analysis provided a useful method to examine the seasonal succession of phytoplankton assemblages in the TGR, and these findings provided strategic insight for the water-quality management in the post-TGDP period.

1. Introduction

Phytoplankton assemblages are extremely sensitive to environmental changes in most large temperate lakes and reservoirs (Reynolds, 2006). Interactions between anthropogenic and natural drivers can strongly affect phytoplankton community structure, thereby resulting in periodic and predictive phytoplankton succession (e.g. critical transition from cyanobacterial bloom to green algal bloom) at an annual scale (Litchman et al., 2010; Thomas et al., 2018). As such, the seasonal succession of phytoplankton assemblages is generally considered as an indicator of aquatic ecosystem changes at different spatiotemporal

scales (Domingues et al., 2007; Wu et al., 2016; Yang et al., 2017). Comprehensively ascertaining the competition and co-existence of different bloom-dominating groups in eutrophic water bodies and their responses to environmental drivers is an important task for ecologists, water resource managers and policy makers (Ji et al., 2017; Zhu et al., 2013).

The seasonal fluctuation of phytoplankton biomass has been well characterised in algal ecological dynamic models, such as plankton ecology group (Sommer et al., 1986), phytoplankton responses to environmental change (Reynolds and Irish, 1997) and simulation of an analytical lake models (Benndorf and Recknagel, 1982), which focus on

Abbreviations: TGDP, Three Gorges Dam Project; TGR, Three Gorges Reservoir; HJ-1, Huan Jing 1; CCD, charge-coupled device; Chl_a, chlorophyll *a*; R_{rs}, remote sensing reflectance; PSD, phytoplankton succession date; CCRSDA, China Centre for Resources Satellite Data and Application; 6S model, second simulation of the satellite signal in the solar spectrum; CCI, Cyano-Chlorophyta index; CWT, continuous wavelet transform; a, approximation sub-band; d, detail sub-band; R², determination coefficient; N/P, total nitrogen/total phosphorus

* Corresponding author. Chongqing Institute of Green and Intelligent Technology, Chinese Academy of Sciences, Chongqing, 400714, China.

E-mail addresses: zhoubotian@cigit.ac.cn (B. Zhou), shankun@cigit.ac.cn (K. Shan).

<https://doi.org/10.1016/j.jenvman.2019.06.035>

Received 15 November 2018; Received in revised form 10 June 2019; Accepted 10 June 2019

0301-4797/© 2019 Elsevier Ltd. All rights reserved.

the biotic and abiotic drivers of phytoplankton succession. On the basis of these models, the phytoplankton community structure should demonstrate annual periodic dynamics. For example, two evident peaks within a year (i.e. a cyanobacterial bloom in spring and a eukaryotic algal bloom in summer) should emerge in the phytoplankton biomass in eutrophic lakes and reservoirs (Carey et al., 2016). A unimodal phytoplankton biomass within a year (i.e. a cyanobacterial or eukaryotic algal bloom during the transition from spring to summer) should be observed in oligotrophic water bodies due to nutrient limitation (Sommer et al., 2012). However, the limited number of sampling sites has proven that these algal ecological dynamic models cannot elucidate the spatiotemporal pattern of phytoplankton succession, especially in a large water body where various algal groups dominate in different periods or co-exist in patches (Shi et al., 2015). Although computational aquatic ecosystem dynamic models have also been extensively utilised in the rapid analysis of the spatiotemporal dynamics of the phytoplankton community structure, this strategy involves skill-intensive, labour-intensive and time-consuming processes (Wallace and Hamilton, 2000). These limitations illustrate the need to develop techniques that can extend the traditional models to characterise the regional-scale dynamics of phytoplankton assemblages rather than by only understanding the field-scale phytoplankton succession.

Remote sensing overcomes some limitations of traditional models and exhibits the potential to delineate the spatial distribution of individual algal blooms using different remote sensor data, such as Terra/Aqua MODIS, Landsats ETM+/OLI, Envisat MERIS, Sentinel-2A MSI, Huan Jing 1 (HJ-1) charge-coupled device (CCD) and airborne AISA images (Matthews and Odermatt, 2015; Oyama et al., 2015; Page et al., 2018; Song et al., 2012; Xing and Hu, 2016; Zhang et al., 2011). In the previous decade, remote sensing has improved the comprehension for distinguishing the diagnostic pigments of different bloom-dominating groups in inland waters [e.g. chlorophyll *a* (Chl*a*) and phycocyanin] (Kudela et al., 2015) and in coastal waters (e.g. fucoxanthin and peridinin) (Cannizzaro et al., 2008; Shang et al., 2014). However, the subtle remote sensing reflectance (R_{rs}) changes in phytoplankton succession cannot be examined by only using remote sensor data with uncertain time interval caused by the complex climate conditions. This limitation can be partially attributed to the difficulties of extracting weak R_{rs} characteristics of phytoplankton community structure. The lack of time series analysis for the growth and extinction of group-specific blooms is another possible limitation for remote examination of phytoplankton succession.

A time series dataset is often nonlinear and non-stationary due to various frequencies, annual variations, interannual fluctuations and noise (Deng and Wang, 2017; Verma and Dutta, 2012). Numerous methodologies are available for decomposing time series and examining abrupt changes. Such methodologies are statistics-based, such as TIMESAT, which is a software for analysing time series of remote sensor data (Jönsson and Eklundh, 2004), and breaks for additive seasonal and trend (Verbesselt et al., 2010) and Fourier-based tools, such as wavelet transform (Wagenseil and Samimi, 2006). The current study attempted to introduce time series analysis for examining the variations in the R_{rs} spectrum in response to the seasonal succession of phytoplankton assemblages.

Over the past decades, cyanobacterial and eukaryotic algal (e.g. green algae) blooms have occurred in several tributaries in the Three Gorges Reservoir (TGR) in China (Liu et al., 2012; Zeng et al., 2006). Therefore, TGR provides an excellent experimental site and data source for exploring the temporal pattern of phytoplankton succession. The objectives of this study are as follows: (1) to establish a spectral characteristics time series that indicates cyanobacterial and green algal blooms, (2) to develop a time series analysis method that identifies the phytoplankton succession date (PSD) between the two phenotypes of blooms at an appropriate time scale and (3) to survey the temporal pattern and environmental drivers of phytoplankton succession in the TGR.

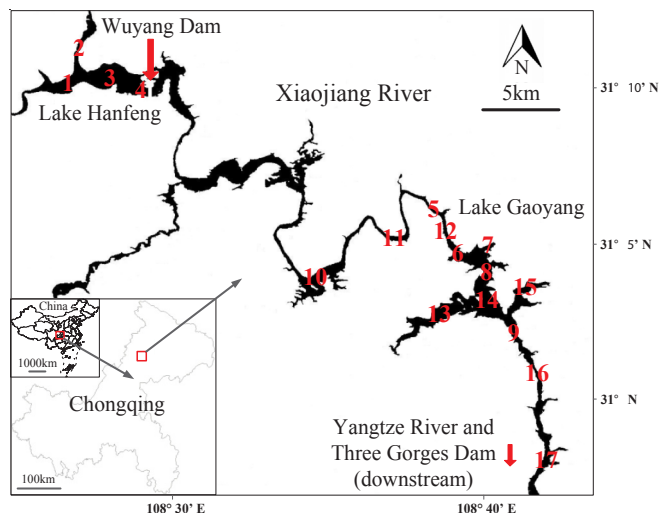


Fig. 1. Locations of Lakes Gaoyang and Hanfeng (Sampling sites 1–9 and 1–17 for ship surveys in 2016 and 2018, respectively).

2. Materials and methods

2.1. Study area

The study area included Lakes Gaoyang and Hanfeng along the Xiaojiang River, which is a primary tributary in the TGR (Fig. 1). In the previous decade, eutrophication was observed in the Xiaojiang River because of biological sewage and agricultural and industrial wastewaters from upstream rivers and the Yangtze River due to backwater effect. Recurrent algal blooms occurred frequently after the construction of the Three Gorges Dam Project (TGDP) (Li et al., 2012; Xiao et al., 2016).

As a Yangtze River-connected lake, Lake Gaoyang is located at the Xiaojiang River backwater area formed by the TGDP and approximately 30 km downstream from Wuyang Dam. Lake Hanfeng is located upstream of Lake Gaoyang in the Xiaojiang River and originated from the water storage of Wuyang Dam since May 2012. After 5 years of Wuyang Dam commissioning, the water level in Lake Hanfeng has been stabilised at beyond 169 m to relieve the ecological problems in the water-level fluctuation zone of 145–175 m in the Xiaojiang River (Yang et al., 2017).

2.2. In situ data collection

Ship surveys were conducted 13 times during March–October of 2016 and May–August of 2018 in the Xiaojiang River. The surveys were performed between 10:30 and 11:30 am Beijing time, which was consistent with the overflight timing of HJ-1 A/B satellites. Eight cruises sailed in Lake Gaoyang but only five in Lake Hanfeng due to shallow water, which prevented sailing activities in the summer of 2016. Cyanobacterial and green algal blooms were observed during the sampling periods.

Sampling sites 1–17 with various eutrophication grades are located along the Xiaojiang River (Fig. 1). We collected 33 and 51 water samples at approximately 0.25 m under the water surface during (2016) and after (2018) the Wuyang Dam commissioning, respectively. Half of the water sample was filtered using Whatman GF/C fibreglass filters with pore size of 1.2 μm for the laboratory analysis of Chl*a* (Sartory and Grobbelaar, 1984). We defined the Chl*a* concentration beyond 10 $\mu\text{g/L}$ as a bloom following Brian and Malcolm (2002). Approximately 1 L of water sample was collected by using a polymethyl methacrylate sampler and preserved with acid Lugol's solution (1% final concentration). After 48 h of sedimentation in the dark, the supernatant was removed,

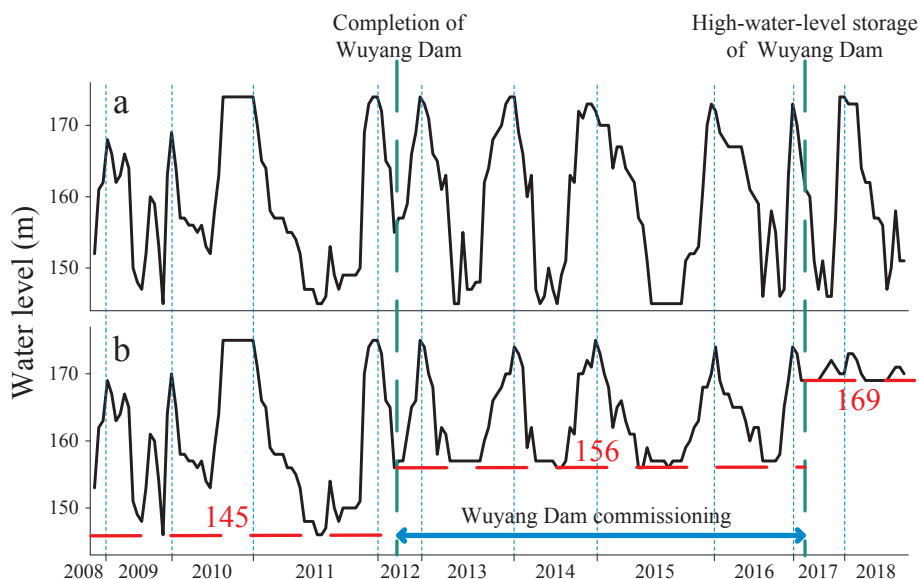


Fig. 2. A 10-year time series of water levels in Lakes a) Gaoyang and b) Hanfeng corresponding to HJ-1 CCD image acquisition date.

and 0.1 ml of homogeneous remainder was placed in a 20 mm × 20 mm settling chamber to quantify cell counting at the algal group level using a CX31 microscope (Olympus, Japan), following the methods described by Hu and Wei (2006) and Utermöhl (1958). We defined the bloom-dominating group as single algal group with a relative cell counting that exceeds 60% of the total phytoplankton population (Xiao et al., 2016). These results were used to calibrate and validate the remote examination of phytoplankton succession.

Water levels in Lakes Gaoyang and Hanfeng referred to the water-level data under and in front of Wuyang Dam. These data were provided by the integrated automation adjustment system of Wuyang Dam. Air temperature in the study area was acquired from the weather service data from the Chongqing Municipal Bureau of Meteorology. Water chemical parameters including pH, total nitrogen and total phosphorus were obtained from the Chongqing Municipal Bureau of Ecology and Environment. Fig. 2 and Table 1 showed the annual and interannual water-level fluctuations and limnological characteristics in Lakes Gaoyang and Hanfeng.

2.3. Satellite images

This study selected HJ-1 CCD images as remote sensor data downloaded from the China Centre for Resources Satellite Data and Application (CCRSDA) (<http://www.cresda.com/CN/>). The spatial

resolution of a CCD imagery is 30 m, and the revisit interval of HJ-1 A/B satellites is 2 d. A 10-year time series (September 2008–August 2018) of 286 cloud-free CCD images was available for monitoring algal blooms in Lakes Gaoyang and Hanfeng using four multispectral bands (i.e. blue band, 430–520 nm; green band, 520–600 nm; red band, 630–690 nm; and near-infrared band, 760–900 nm). Thirteen of these CCD images were captured at the same time as our ship surveys.

HJ-1 CCD images were pre-processed using MATLAB 2014a and ENVI 4.8 in three steps, namely, radiometric calibration, geometric rectification and atmospheric correction. Radiometric calibration was conducted using the calibration coefficient of each CCD band provided by the CCRSDA. Geometric rectification was conducted with a rectified ETM + image. Geometric errors were limited to less than one pixel. The second simulation of the satellite signal in the solar spectrum (6S model), which has been widely applied in accurate remote monitoring of lakes and reservoirs, was selected as an atmospheric correction method. The 6S model not only uses bidirectional reflectance distribution function in the radiative transfer calculations but also considers aerosol scattering, gas absorption and Lambert radiator (Vermote et al., 1997). The input parameters, such as the altitude of target and atmospheric and aerosol models, of the 6S model referred to the geometric conditions from the XML file of the CCD image and the standard modes provided by the 6S model based on the geographic and seasonal information. The response function of each CCD band was obtained

Table 1
Limnological characteristics of Lakes Gaoyang and Hanfeng during and after the Wuyang Dam commissioning.

Sampling period	2016		2018	
	Lake Gaoyang	Lake Hanfeng	Lake Gaoyang	Lake Hanfeng
Study area	Mean (minimal–maximal)		Mean (minimal–maximal)	
Water level (m)	162 (145–174)	164 (146–175)	160 (145–174)	172 (169–175)
Lake area (km ²)	7.5 (7–8.5)	5.5 (4.5–7)	7.2 (6.5–8.4)	7 (6.9–7.1)
Water depth (m)	6.5 (1–12)	7 (0–20)	6.4 (0.8–11.5)	13 (6–20)
Turbidity (NTU)	20.2 (3.4–62.3)	28.9 (8.4–72.6)	14.6 (1.7–42.8)	25.2 (6.9–60.1)
Chla (µg/L)	19.47 (0.89–226.51)	5.62 (0.2–22.67)	10.32 (0.27–89.75)	25.23 (14.8–57.46)
Phycocyanin (µg/L)	1.2 (0.03–8.83)	0.29 (0.08–1.07)	0.84 (0.04–5.41)	2.97 (0.16–4.1)
pH	8.57 (7.06–9.53)	8.29 (7.79–8.29)	8.02 (7.19–8.78)	8.45 (7.69–8.84)
Dissolve oxygen (mg/L)	10.36 (4.81–22.88)	8.49 (5.74–11.5)	12.1 (5.29–26.43)	6.31 (4.82–9.66)
Ammonia nitrogen (mg/L)	0.104 (0.09–0.11)	0.15 (0.1–0.17)	0.124 (0.09–0.17)	0.132 (0.09–0.159)
Total phosphorus (mg/L)	0.09 (0.05–0.17)	0.11 (0.05–0.29)	0.07 (0.02–0.11)	0.15 (0.06–0.36)
Total nitrogen (mg/L)	1.26 (0.64–1.85)	1.48 (0.31–2.47)	0.89 (0.56–1.35)	1.79 (1.17–2.64)

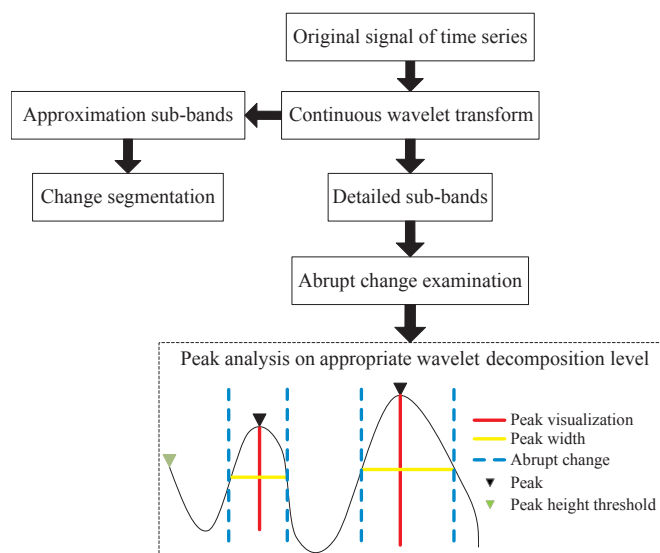


Fig. 3. Flowchart of CWT-based peak analysis. After the original time series is decomposed into detailed sub-bands, peak analysis can be used in examining the abrupt change points in the time series.

from the CCRSDA. Ground reflectance was measured as the water surface R_{rs} . Apparent radiance was based on the radiance values of CCD image. In this study, the validation of atmospheric correction was analysed by consistency evaluation among the water surface R_{rs} derived from the 6S model at the adjacent sampling sites, and by cross-validation analysis with R_{rs} standard products of Landsat 8 OLI image, respectively.

To remove adjacency effect by land, we extracted the valid water surface R_{rs} of each CCD band within a 3×3 pixel box around the sampling site (Bailey and Werdell, 2006). If the valid pixel number was ≥ 5 , then we estimated the water surface R_{rs} and standard deviation for four CCD bands at the sampling site. After deleting invalid values (beyond 1.5 standard deviation), mean water surface R_{rs} could be calculated based on the remaining valid values within the 3×3 pixel box.

2.4. Distinguishing algorithm for bloom-dominating groups

Algal bloom state has low transparency and may carry narrow fringes of floating vegetation on the shallow side. The red and near-infrared reflectance can be considerably enhanced, as shown by the level of algae accumulation on the water surface (Zhang et al., 2012). Thus, algal bloom identification was feasible by estimating the Chla concentration and assessing whether retrieval value $\geq 10 \mu\text{g/L}$. Zhou et al. (2017) developed and validated the two-, three- and four-CCD band combinations and band-ratio to retrieve Chla in the TGR (Zhou et al., 2017). In the current study, the optimum band combination in Eq. (1) was selected to calibrate a retrieval model of Chla under rapid change conditions in the phytoplankton community structure. On the basis of the algal bloom definition in this study, Chla time series was used to determine the bloom periods, which were determined as the summation of all phases with mean Chla $\geq 10 \mu\text{g/L}$ from the corresponding sampling sites on each corrected CCD image from September 2008 to August 2018.

$$\text{Chl}\alpha = 56.4 \times (\text{CCD}3^{-1} - \text{CCD}4^{-1}) \times \text{CCD}4 + 13.5 \quad (1)$$

where CCD3 and CCD4 were mean water surface R_{rs} of red and near-infrared bands within 3×3 pixel box around the sampling site, respectively.

Lakes Gaoyang and Hanfeng can assume two distinct states with respect to primary producers by in situ observations during our ship surveys, that is, cyanobacteria and green algae at the algal group level.

To distinguish the two bloom-dominating groups, we created a spectral index to indicate the distinctive differences in the shapes and magnitudes of their R_{rs} spectra. The ratio of peak–valley depths between reflectance peaks at 570 nm (green band) and 640 nm (red band) and the reflectance valleys of cyanobacterial cells located at 475–500 nm (blue band) and 620–640 nm (red band) represented as the Cyanobacteria-Chlorophyta index (CCI) in Eq. (2) (Zhou et al., 2018). The CCI threshold was effective for distinguishing cyanobacterial (high CCI value) and green algal (low CCI value) blooms. This threshold represented the mid-point between the lowest CCI measured in the cyanobacterial bloom states and the highest CCI for green algal blooms. We determined the criterion and realised that Chla and CCI thresholds indicate the two bloom-dominating groups in terms of spatial distribution.

$$\text{CCI} = (\text{CCD}1 - \text{CCD}3)/(\text{CCD}2 - \text{CCD}3) \quad (2)$$

where CCD1, CCD2 and CCD3 were mean water surface R_{rs} of blue, green and red bands within 3×3 pixel box around the sampling site, respectively.

2.5. Wavelet decomposition model

Statistics-based time series analysis requires a priori basis function to fit some components and effectively represents the time series characteristics in certain phases but not in other segments of a non-stationary time series (Flandrin et al., 2004). Continuous wavelet transform (CWT), as a Fourier-based method, provides a flexible approach for examining the different change forms of time series by scaling a wavelet base function and quantifying a wavelet coefficient at each possible scale (Huang et al., 1998; Khorrami and Moavenian, 2010). An oscillatory function can resolve the temporal location and pinpoint where the correspondence between the spectral signature of phytoplankton community structure and mother wavelet is high. Consequently, we utilised a routine written in MATLAB 2014a of the CWT to examine the seasonal fluctuations in the mean CCI time series that were established from the corresponding sampling sites on each corrected CCD image during the bloom periods of 2008–2018.

The decomposition of CWT can be represented as a tree (Fig. 3), where the CCI time series is passed through low and high filters, yielding approximation (a) and detailed (d) sub-bands (Mallat, 1999). The approximation sub-bands contained the low-frequency components of CCI time series maintained a periodic tendency due to the growth and extinction of bloom-dominating groups. By contrast, the detailed sub-bands contained the high-frequency components of CCI time-varying trend, which enabled the capture of subtle abrupt changes in phytoplankton succession.

2.6. Peak analysis of CCI decomposition sub-bands

In this study, CWT-based peak analysis included two main steps. Firstly, the appropriate CCI detailed sub-band and peak height threshold that must be selected at which the abrupt change points of the CCI time-varying trend can be detected. Secondly, the wavelet peak width was calculated to examine the temporal pattern in the seasonal succession of phytoplankton assemblages.

Depending on the in situ observation of phytoplankton dynamics, the appropriate CCI detailed sub-band was flexible to estimate the persistent periods of bloom-dominating groups, that is, by retaining to the phenology of the algal group (Soleymani et al., 2017). The peak height threshold was ascertained by selecting the low peak height near the two endpoints of the selected CCI detailed sub-band.

Wavelet peak visualisation was used to calculate the wavelet peak width from the selected CCI detailed sub-band. The visualisation of a wavelet peak was the minimal vertical distance from the peak to the local minimum on either side of the peak before arriving at the endpoints or another higher peak (Fig. 3). The wavelet peak width was

determined as the distance between the two points on either side of the peak, where the selected CCI detailed sub-band intercepted the horizontal line through the midpoint of wavelet peak visualisation. The PSDs could be defined as the extreme points of wavelet peak width. A new phytoplankton succession was only started if the adjacent wavelet peak exceeded the peak height threshold.

3. Results

3.1. Distinguishing result of bloom-dominating groups

Microscopic analysis revealed that 37 water samples satisfied the criteria of algal bloom label, that is, the relative cell counting of the single bloom-dominated groups exceeded 60%. Majority of the bloom-dominated groups in Lakes Gaoyang and Hanfeng were cyanobacteria and green algae, respectively.

We utilised 13 corrected CCD images, which coincided in time with water sampling, to evaluate the interpretations of the proposed method to distinguish cyanobacterial and green algal blooms. The Chla [determination coefficient (R^2) and root-mean-square error between measured values of Chla derived from laboratory analysis and CCD-derived retrieval values of Chla were 0.74 and 7.1 $\mu\text{g/L}$, respectively] and CCI thresholds worked well in identifying the bloom-dominating groups. The CCI values for 26 water samples with cyanobacterial bloom label derived from corresponding 3×3 pixel box around the sampling sites were in the range of 0.027–0.187. By contrast, the CCI for green algal bloom samples decreased to < 0.022 . Consequently, the CCI of 0.0245 could be the threshold to distinguish the two bloom-dominating groups in the study area.

3.2. Time-varying trend construction for the two typical bloom-dominating groups

For the bloom period of 2016, the CCI curves shown in Fig. 4 represented the two typical phytoplankton succession patterns in Lake Gaoyang. The two classes of CCI time-varying trends showed higher CCI in spring than in other seasons and most of negative CCI in summer. The CCI curve of Class I was normally found in the river channel with remarkable hydrodynamic changes. By contrast, the CCI time-varying trend in Class II was generally observed in the bays under relatively stable hydrodynamic conditions. The magnitude and change pattern of the CCI curves, which indicated the competition and co-existence between cyanobacteria and green algae, might vary with space and time due to variable hydrodynamics and phenology of the bloom-dominating groups.

In the present study, a 10-year time series of Chla was constructed to determine the bloom periods (Fig. 5). As wavelet base function for the CWT, daubechies 5 mother wavelet passed the test because it could provide a good balance between the frequency and time localisation at the abrupt change points of CCI time-varying trends.

An appropriate level must be selected to guarantee that noise would not result in many false positives. The CWT-based peak analysis showed that the peak height threshold on the d5 (Fig. 5), where the

phytoplankton succession became apparent, was indicative of such changes. The analysis revealed whether peak height threshold would allow the further examination of fine-scale abrupt changes based on whether the wavelet peak width ranges contained the collection timing of cyanobacterial bloom samples.

3.3. Comparative analysis of the temporal pattern of PSDs

Table 2 showed that the horizontal distances between the first and second PSDs examined by CWT-based peak analysis on the d5 was a good estimator for accurately examining the persistent periods of the bloom-dominating groups. For example, the temporal difference between the PSDs derived from CWT-based peak analysis and area replacement estimation [cited from Zhou et al. (2018)] was 7–12 d (Fig. 6a–c) in Lake Gaoyang in 2016. In most eutrophic large reservoir with two evident peaks of a cyanobacterial biomass in spring and a eukaryotic algal biomass in summer, water sampling once a month was sufficient to provide a good overall examination of the phytoplankton succession (Pobel et al., 2011). Thus, the time difference of 7–12 d exhibited relatively acceptable accuracy compared with the sampling interval (15–30 d) of conventional monitoring for algal blooms, persistent period (20–90 d) of the single bloom-dominated group and bloom period (80–160 d). In Fig. 6a and d, the comparative analyses amongst the PSDs derived from the two examining methods and microscopic analysis results of the bloom-dominating groups further illustrated the applicability of the proposed method for examining the phytoplankton succession during the bloom periods of 2008–2018.

4. Discussion

Even though 10-year remote sensing images are not as long as those by many on-site monitoring for water quality, time-varying trends from satellite-derived data can enable reservoir managers to detect the potential drivers of seasonal succession of phytoplankton assemblages. Our efforts established the linear relationships between PSDs and abiotic factors to interpret the roles of hydrodynamic alteration (water level), climatic change (air temperature) and water chemical parameters [pH and total nitrogen/total phosphorus (N/P) ratio] on phytoplankton succession in the backwater area of the TGR (Xiao et al., 2016). The different temporal patterns were observed from April to August during 2008–2018. Fig. 7 showed that positive correlations were found between mean water level, N/P ratio and first PSD, but negative correlations was expectedly found between pH and first PSD in Lake Gaoyang. By contrast, second PSD had a strong positive relationship with pH, albeit negatively significant with N/P ratio. In fact, the two types of PSDs corresponded to the rise phase of green algal and cyanobacterial blooms, respectively. The seasonal shifts in bloom-dominating groups might be attributed to their relative eco-physiology strategy, because previous studies revealed cyanobacteria blooms resulted in high pH and low N/P ratio (Shan et al., 2019; Xie et al., 2003). It was partly in agreement with the findings in the recent MODIS-derived phytoplankton phenology (Shi et al., 2019).

Meanwhile, air temperature was found to have a hump-shaped

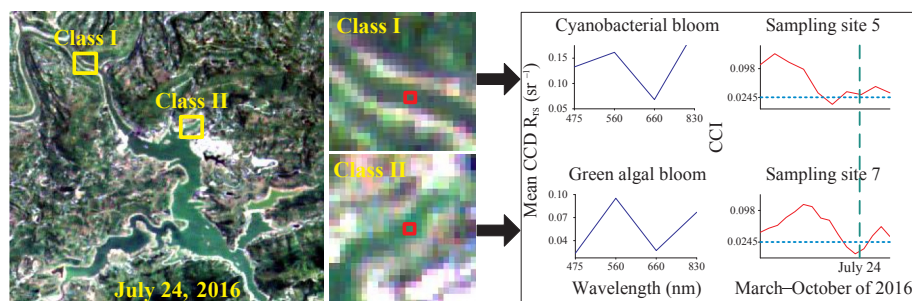


Fig. 4. Typical examples of the two classes of CCI time-varying trend in Lake Gaoyang during the sampling period of 2016. Cyanobacterial and green algal blooms were observed in the yellow rectangular boxes around Sampling sites 5 and 7, respectively. The red rectangular box contained 3×3 CCD pixels around the sampling site in the middle of river or bay. Only mean CCD R_{rs} in the red rectangular box was used to remove adjacency effect by land. The vertical green and horizontal blue dashed lines indicated CCD image acquisition date and CCI threshold, respectively.

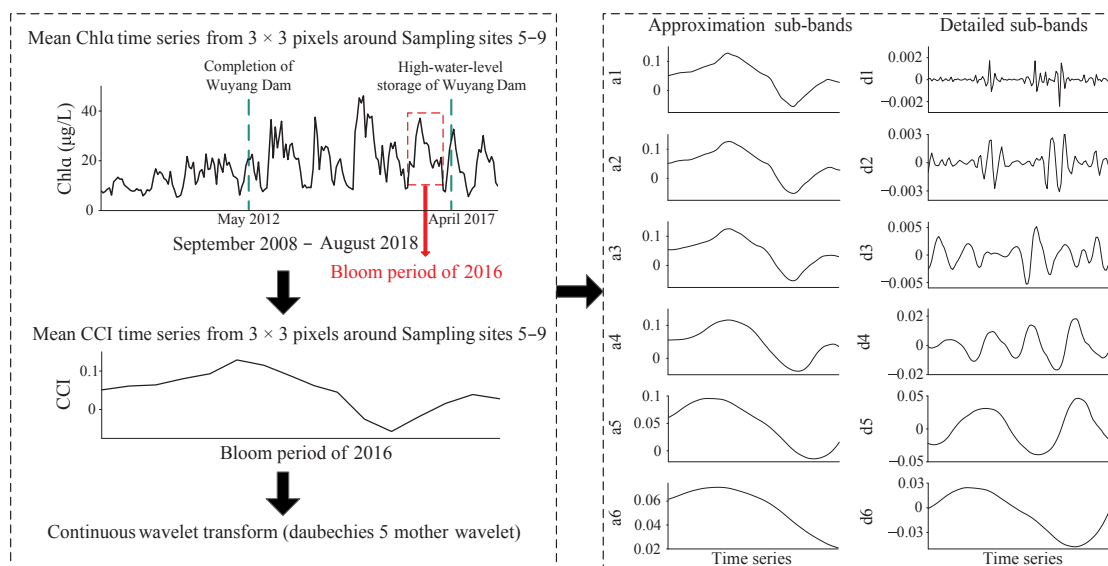


Fig. 5. A Chla time series derived from CCD images in Lake Gaoyang from 2008 to 2018 and the corresponding CCI decomposition sub-bands during the bloom period of 2016.

Table 2
Comparison for sampling timing and persistent period of two bloom-dominating groups.

Bloom-dominating group	Number of labelled water samples	Number in examined persistent periods	Comments
Cyanobacteria	26	24	2 miss examination due to edge effects
Green algae	11	13	2 redundant examination due to edge effects

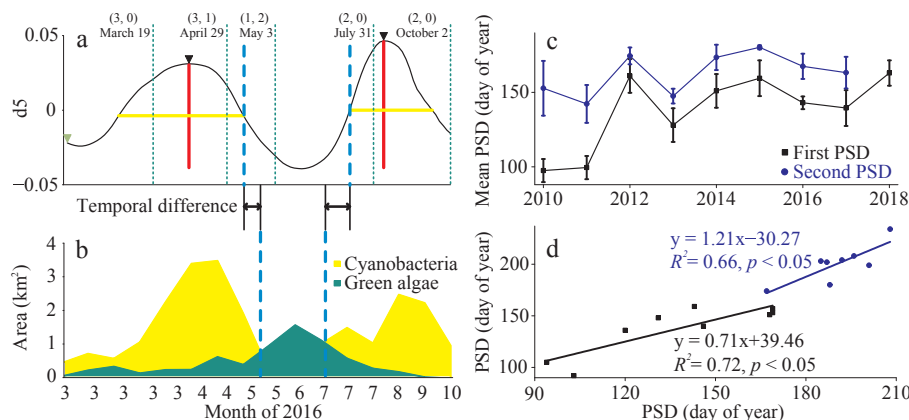


Fig. 6. Coherence assessment for the two examining methods of PSDs in Lake Gaoyang. a) CWT-based peak analysis on the selected CCI detailed sub-band [for interpretation of the references to colour and symbol was referred to Fig. 3; vertical green dash lines indicated the date of ship surveys and the corresponding microscopic analysis results of the bloom-dominating groups, that is, label numbers (in the brackets) of cyanobacterial and green algal blooms in water samples collected from Sampling sites 5–9]; b) Area replacements between the two phenotypes of blooms cited from Zhou et al. (2018) (vertical blue dash lines indicated the PSDs); c) Mean PSDs derived from CWT-based peak analysis and area replacement estimation; and d) X- and Y-axis represented the PSDs derived from CWT-based peak analysis and area replacement estimation, respectively.

relationship with the first PSD. This result contradicted the controlled experiment by Lürling et al. (2013), who suggested that the competitive advantage of cyanobacteria over green algae can more likely be attributed to other factors or synergistic effects rather than to temperature alone at relatively high temperatures. Using satellite and in situ observations, the relationship analyses were conducted to pinpoint the correlations between water-level fluctuation and bloom dynamics in

Lake Gaoyang during the bloom periods of 2008–2018 (Table 3). The high correlation between water-level fluctuation and Chla suggested that the growth and extinction of bloom-dominating groups were accelerated by the extended hydraulic retention time (O’Farrell et al., 2011; Yu et al., 2018). During the water storage period from October to February the following year, along with the rise in water level (165–175 m), the decrease in CCI fluctuation was caused by a relatively

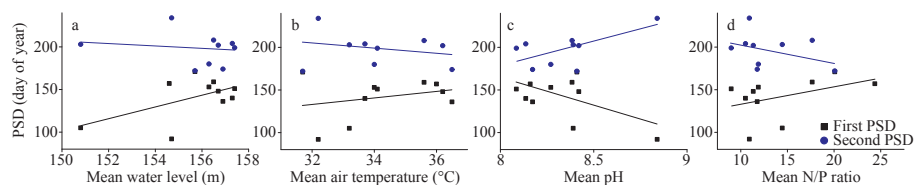


Fig. 7. Linear correlations between the PSDs and mean environmental variables in Lake Gaoyang from April to August during 2008–2018. a) Mean water level [first PSD ($R^2 = 0.31$, $p = 0.042$), second PSD ($R^2 = 0.05$, $p = 0.539$)]; b) Mean air temperature [first PSD ($R^2 = 0.03$, $p = 0.659$), second PSD ($R^2 = 0.08$, $p = 0.403$)]; c) Mean pH [first PSD ($R^2 = 0.33$, $p = 0.083$), second PSD ($R^2 = 0.36$, $p = 0.088$)]; Mean N/P ratio [first PSD ($R^2 = 0.18$, $p = 0.221$), second PSD ($R^2 = 0.1$, $p = 0.405$)].

Table 3
Statistics of water-level fluctuation and algal blooms in Lake Gaoyang during the bloom periods of 2008–2018.

Year	Duration of water-level rise [daily rise and water level vs. Chla (R^2)]	Duration of water-level fall [daily fall and water level vs. Chla (R^2)]	Persistent period (cyanobacterial and green algal blooms)
2008	–	–	–
2009	55 d (0.65 m/d and 0.51)	60 d (0.3 m/d and 0.89)	60 d (58 d and 2 d)
2010	35 d (0.31 m/d and 0.55)	75 d (0.06 m/d and 0.63)	182 d (39 d and 143 d)
2011	69 d (0.46 m/d and 0.64)	133 d (0.15 m/d and 0.35)	190 d (91 d and 99 d)
2012	52 d (0.23 m/d and 0.62)	63 d (0.16 m/d and 0.57)	198 d (170 d and 28 d)
2013	70 d (0.21 m/d and 0.86)	84 d (0.35 m/d and 0.51)	240 d (201 d and 39 d)
2014	67 d (0.42 m/d and 0.73)	72 d (0.25 m/d and 0.46)	210 d (160 d and 50 d)
2015	69 d (0.38 m/d and 0.78)	78 d (0.28 m/d and 0.32)	206 d (157 d and 49 d)
2016	57 d (0.4 m/d and 0.84)	103 d (0.21 m/d and 0.33)	216 d (151 d and 65 d)
2017	89 d (0.31 m/d and 0.85)	85 d (0.32 m/d and 0.82)	218 d (163 d and 55 d)
2018	10 d (0.8 m/d and 0.78)	90 d (0.19 m/d and 0.81)	143 d (109 d and 34 d)

In the statistics, the events with total and daily water-level fluctuation < 5 m and 0.15 m/d were ignored, except for 2010. Chla concentration and bloom persistent period were retrieved from the CCD image time series.

stable hydrodynamic condition. An opposite scenario occurred in the water discharge period (the corresponding range of water level was 155–165 m from March to June), which resulted in a substantial CCI fluctuation (Fig. 4).

It was reported that, cyanobacterial blooms occurred in Lake Gaoyang during the water discharge period prior to October 2010. Then, water level in the TGR initially reached 175 m, forming a water-level fluctuation zone of 145–175 m. Accompanied by hydrodynamic dynamics, some eukaryotic algae gradually started competing with cyanobacteria (Yang et al., 2018). The bloom duration in 2010 extended to more than three times that of 2009 (Table 3). As far as the backwater area in the Xiaojiang River was concerned, the operation of Wuyang Dam since May 2012 formed a so-called water-level linkage mechanism with Three Gorges Dam, by which the summer flood inflowing from Lake Hanfeng into Lake Gaoyang was controlled. During the low-water-level period (the corresponding range of water level was 145–155 m from July to September), an intermittent water-level rise would trigger critical transition from green algal bloom to cyanobacterial bloom.

Given the high-water-level storage (water level beyond 169 m in Lake Hanfeng after April 2017) of Wuyang Dam, the low nutrient concentration and high stability of water column in Lake Gaoyang due to a remarkable decline in the upstream inflow resulted in the distinct reductions of Chla concentration and bloom duration during the bloom period of 2018 (Fig. 5 and Table 3). The limit primary production might alter the critical criteria of phytoplankton succession. For example, cyanobacteria presented stronger capability than green algae to adapt to water-level linkage mechanism during the low-water-level period, because cyanobacteria are typically associated with high temperature and water column stability (Ji et al., 2017; Paerl and Huisman, 2009; Yang et al., 2016). The absence of second PSD in Lake Gaoyang in 2018 was an important difference compared with that of 2009–2017.

In this study, we concluded that the high-water-level storage of Wuyang Dam showed a considerable positive effect on algal bloom prevention in the Xiaojiang River backwater area. The water-level linkage mechanism between the Wuyang and Three Gorges Dams is considered as the key contributor to bloom dynamics and the main indicator of PSDs, thereby providing a basis of the influence of the temporal pattern of phytoplankton succession in the TGR. Although remote sensing together with CWT-based peak analysis provided a useful screening tool for time-series distribution of blooms, their relative effectiveness should be further evaluated in other tributaries of the TGR. We could expect that the ecological scheduling operation based on the water-level linkage mechanism amongst the cascade dams and Three Gorges Dam would continue to mitigate the occurrence of harmful algal blooms and promote the water quality in the TGR.

5. Conclusion

The aquatic ecosystem in the TGR has changed considerably in natural and social environments over the past decades. The ecological scheduling operation for algal bloom prevention must urgently characterise the seasonal succession of phytoplankton assemblages at a fine temporal scale. This study comprehensively analysed a satellite-derived CCI time series to examine the PSDs between cyanobacterial and green algal blooms in the TGR. For this purpose, CWT-based peak analysis flexibly determined the appropriate CCI detailed sub-band and the corresponding peak height threshold and peak width. The analysis results provided an effective channel to closely examine the temporal pattern in phytoplankton succession and its complex responses to water-level linkage mechanism. These results demonstrated that the proposed method is a considerable knowledge base for the on-going monitoring of harmful algal blooms. With the aid of CWT-based peak analysis, reservoir managers can formulate well-directed decisions in implementing countermeasures for harmful algal blooms in the post-TGDP period.

Acknowledgments

This study was conducted with the support of the National Science and Technology Major Project of China (2014ZX07104-006), the Chongqing Science and Technology Innovation Special Project for Social Livelihood (Y61Z030A10) and the National Natural Science Foundation of China (51609229). We thank Jianrong Ma, Zhaofei Wen, Hong Li and Guofeng Yang for their help in the field experiments. We are grateful to the reviews for their constructive comments.

References

- Bailey, S.W., Werdell, P.J., 2006. A multi-sensor approach for the on-orbit validation of ocean color satellite data products. *Remote Sens. Environ.* 102, 12–23.
- Benndorf, J., Recknagel, F., 1982. Problems of application of the ecological model SALMO to lakes and reservoirs having various trophic states. *Ecol. Model.* 17, 129–145.
- Brian, A.W., Malcolm, P., 2002. *The Ecology of Cyanobacteria: Their Diversity in Time and Space*. Kluwer Academic Publishers, New York.
- Cannizzaro, J.P., Carder, K.L., Chen, F.R., Heil, C.A., Vargo, G.A., 2008. A novel technique for detection of the toxic dinoflagellate, *Karenia brevis*, in the Gulf of Mexico from remotely sensed ocean color data. *Cont. Shelf Res.* 28, 137–158.
- Carey, C.C., Hanson, P.C., Lathrop, R.C., Amand, A.L.S., 2016. Using wavelet analyses to examine variability in phytoplankton seasonal succession and annual periodicity. *J. Plankton Res.* 38, 27–40.
- Deng, W., Wang, G., 2017. A novel water quality data analysis framework based on time-series data mining. *J. Environ. Manag.* 196, 365–375.
- Domingues, R.B., Sobrino, C., Galvao, H., 2007. Impact of reservoir filling on phytoplankton succession and cyanobacteria blooms in a temperate estuary. *Estuar. Coast Shelf Sci.* 74, 31–43.
- Flandrin, P., Goncalves, P., Rilling, G., 2004. Detrending and denoising with empirical mode decompositions. In: *The 2004 European Signal Processing Conference (EUSIPCO 2004)*, pp. 1581–1584.
- Huang, N., Shen, Z., Long, S., Wu, M., Shih, H., Zheng, Q., Yen, N., Tung, C., Liu, H., 1998.

- The empirical mode decomposition and the Hilbert spectrum for non-linear and non-stationary time series analysis. *P. Roy. Soc. a-Math. Phys.* 454, 903–995.
- Hu, H., Wei, Y., 2006. *The Freshwater Algae of China: Systematics, Taxonomy and Ecology*. Science Press, Beijing.
- Ji, D., Wells, S.A., Yang, Z., Liu, D., Huang, Y., Ma, J., Berger, C.J., 2017. Impacts of water level rise on algal bloom prevention in the tributary of Three Gorges Reservoir, China. *Ecol. Eng.* 98, 70–81.
- Ji, X., Verspagen, J.M.H., Stomp, M., Huisman, J., 2017. Competition between cyanobacteria and green algae at low versus elevated CO₂: who will win, and why? *J. Exp. Bot.* 68, 3815–3828.
- Jönsson, P., Eklundh, L., 2004. TIMESAT—a program for analyzing time-series of satellite sensor data. *Comput. Geosci.* 30, 833–845.
- Khorrami, H., Moavenian, M., 2010. A comparative study of DWT, CWT and DCT transformations in ECG arrhythmias classification. *Expert Syst. Appl.* 37, 5751–5757.
- Kudela, R.M., Palacios, S.L., Austerberry, D.C., Accorsi, E.K., Guild, L.S., Perez, J.T., 2015. Application of hyperspectral remote sensing to cyanobacterial blooms in inland waters. *Remote Sens. Environ.* 167, 196–205.
- Litchman, E., de Tazanos Pinto, P., Klausmeier, C.A., Thomas, M.K., Yoshiyama, K., 2010. Linking traits to species diversity and community structure in phytoplankton. *Hydrobiologia* 653, 15–28.
- Liu, L., Liu, D., Johnson, D.M., Yi, Z., Huang, Y., 2012. Effects of vertical mixing on phytoplankton blooms in Xiangxi bay of three Gorges reservoir: implications for management. *Water Res.* 46, 2121–2130.
- Li, Z., Wang, S., Guo, J., Fang, F., Gao, X., Long, M., 2012. Responses of phytoplankton diversity to physical disturbance under manual operation in a large reservoir, China. *Hydrobiologia* 684, 45–56.
- Lüring, M., Eshetu, F., Faassen, E.J., Kosten, S., Huszar, V.L., 2013. Comparison of cyanobacterial and green algal growth rates at different temperatures. *Freshw. Biol.* 58 (3), 552–559.
- Mallat, S., 1999. *A Wavelet Tour of Signal Processing*. Academic Press, Burlington, MA, USA.
- Matthews, M.W., Odermatt, D., 2015. Improved algorithm for routine monitoring of cyanobacteria and eutrophication in inland and near-coastal waters. *Remote Sens. Environ.* 156, 374–382.
- O'Farrell, I., Izaguirre, I., Chaparro, G., Unrein, F., Sinistro, R., Pizarro, H., Rodriguez, P., Pinto, P.D., Lombardo, R., Tell, G., 2011. Water level as the main driver of the alternation between a free-floating plant and a phytoplankton dominated state: a long-term study in a floodplain lake. *Aquat. Sci.* 73, 275–287.
- Oyama, Y., Fukushima, T., Matsushita, B., Matsuzaki, H., Kamiya, K., Kobinata, H., 2015. Monitoring levels of cyanobacterial blooms using the visual cyanobacteria index (VCI) and floating algae index (FAI). *Int. J. Appl. Earth Obs. Geoinf.* 38, 335–348.
- Paerl, H.W., Huisman, J., 2009. Climate change: a catalyst for global expansion of harmful cyanobacterial blooms. *Env. Microbiol. Rep.* 1, 27–37.
- Page, B.P., Kumar, A., Mishra, D.R., 2018. A novel cross-satellite based assessment of the spatio-temporal development of a cyanobacterial harmful algal bloom. *Int. J. Appl. Earth Obs. Geoinf.* 66, 69–81.
- Pobel, D., Robin, J., Humbert, J.F., 2011. Influence of sampling strategies on the monitoring of cyanobacteria in shallow lakes: lessons from a case study in France. *Water Res.* 45, 1005–1014.
- Reynolds, C.S., 2006. *The Ecology of Phytoplankton*. Cambridge University Press, UK.
- Reynolds, C.S., Irish, A.E., 1997. Modelling phytoplankton dynamics in lakes and reservoirs: the problem of in-situ growth rates. *Hydrobiologia* 349, 5–17.
- Sartory, D.P., Grobbelaar, J.U., 1984. Extraction of Chlorophyll a from freshwater phytoplankton for spectrophotometric analysis. *Hydrobiologia* 114, 177–187.
- Shan, K., Song, L., Chen, W., Li, L., Liu, L., Wu, Y., Jia, Y., Zhou, Q., Peng, L., 2019. Analysis of environmental drivers influencing interspecific variations and associations among bloom-forming cyanobacteria in large, shallow eutrophic lakes. *Harmful Algae* 84, 84–94.
- Shang, S., Wu, J., Huang, B., Lin, G., Lee, Z., Liu, J., Shang, S., 2014. A new approach to discriminate dinoflagellate from diatom blooms from space in the East China Sea. *J. Geophys. Res.-Oceans* 119, 4653–4668.
- Shi, K., Zhang, Y., Li, Y., Li, L., Lv, H., Liu, X., 2015. Remote estimation of cyanobacteria dominance in inland waters. *Water Res.* 68, 217–226.
- Shi, K., Zhang, Y., Zhang, Y., Li, N., Qin, B., Zhu, G., Zhou, Y., 2019. Phenology of phytoplankton blooms in a trophic lake observed from long-term MODIS data. *Environ. Sci. Technol.* 53, 2324–2331.
- Soleymani, A., Pennekamp, F., Dodge, S., Weibel, R., 2017. Characterizing change points and continuous transitions in movement behaviours using wavelet decomposition. *Methods Ecol. Evol.* 8, 1113–1123.
- Sommer, U., Adrian, R., Domis, L.D., Elser, J.J., Gaedke, U., Ibelings, B., Jeppesen, E., Lüring, M., Molinero, J.C., Mooij, W.M., 2012. Beyond the plankton ecology group (PEG) model: mechanisms driving plankton succession. *Annu. Rev. Ecol. Syst.* 43, 429–448.
- Sommer, U., Gliwicz, Z.M., Lampert, W., Duncan, A., 1986. The PEG-model of seasonal succession of planktonic events in freshwaters. *Arch. Hydrobiol.* 106, 433–471.
- Song, K., Li, L., Li, S., Tedesco, L., Hall, B., Li, Z., 2012. Hyperspectral retrieval of phycocyanin in potable water sources using genetic algorithm-partial least squares (GA-PLS) modeling. *Int. J. Appl. Earth Obs. Geoinf.* 18, 368–385.
- Thomas, M.K., Fontana, S., Reyes, M., Kehoe, M., Pomati, F., 2018. The predictability of a lake phytoplankton community, over time-scales of hours to years. *Ecol. Lett.* 21, 619–628.
- Utermöhl, H., 1958. Zur Vervollkommung der quantitativen Phytoplankton-Methodik. *Mitteilungen der Internationale Vereinigung für Theoretische und Angewandte Limnologie* 9, 1–38.
- Verbesselt, J., Hyndman, R., Newnham, G., Culvenor, D., 2010. Detecting trend and seasonal changes in satellite image time series. *Remote Sens. Environ.* 114, 106–115.
- Verma, R., Dutta, S., 2012. Vegetation dynamics from denoised NDVI using empirical mode decomposition. *J. Indian Soc. Remote* 41, 555–565.
- Vermote, E.F., Tanre, D., Deuze, J.L., Herman, M., Morcrette, J.J., 1997. Second simulation of the satellite signal in the solar spectrum, 6S: an overview. *IEEE Trans. Geosci. Remote* 35, 675–686.
- Wagensel, H., Samimi, C., 2006. Assessing spatio-temporal variations in plant phenology using Fourier analysis on NDVI time series: results from a dry savannah environment in Namibia. *Int. J. Remote Sens.* 27, 3455–3471.
- Wallace, B.B., Hamilton, D.P., 2000. Simulation of water-bloom formation in the cyanobacterium *Microcystis aeruginosa*. *J. Plankton Res.* 22, 1127–1138.
- Wu, Y., Li, L., Zheng, L., Dai, G., Ma, H., Shan, K., Wu, H., Zhou, Q., Song, L., 2016. Patterns of succession between bloom-forming cyanobacteria *Aphanizomenon flos-aquae* and *Microcystis* and related environmental factors in large, shallow Dianchi Lake, China. *Hydrobiologia* 765, 1–13.
- Xiao, Y., Li, Z., Guo, J., Fang, F., Smith, V.H., 2016. Succession of phytoplankton assemblages in response to large-scale reservoir operation: a case study in a tributary of the Three Gorges Reservoir, China. *Environ. Monit. Assess.* 188, 153.
- Xie, L., Xie, P., Tang, H., 2003. Enhancement of dissolved phosphorus release from sediment to lake water by *Microcystis* blooms—an enclosure experiment in a hyper-eutrophic, subtropical Chinese lake. *Environ. Pollut.* 122, 391–399.
- Xing, Q., Hu, C., 2016. Mapping macroalgal blooms in the Yellow Sea and East China Sea using HJ-1 and Landsat data: application of a virtual baseline reflectance height technique. *Remote Sens. Environ.* 178, 113–126.
- Yang, B., He, B., Wang, D., 2017. Hanfeng pre-reservoir commissioning time variation feature of the hydrology and water quality in Three Gorges Reservoir. *Environ. Sci. (Chin.)* 38, 1366–1375.
- Yang, J., Lv, H., Yang, J., Liu, L., Yu, X., Chen, H., 2016. Decline in water level boosts cyanobacteria dominance in subtropical reservoirs. *Sci. Total Environ.* 557–558, 445–452.
- Yang, J.R., Lv, H., Isabwe, A., Liu, L., Yu, X., Chen, H., Yang, J., 2017. Disturbance-induced phytoplankton regime shifts and recovery of cyanobacteria dominance in two subtropical reservoirs. *Water Res.* 120, 52–63.
- Yang, Z., Xu, P., Liu, D., Ma, J., Ji, D., Cui, Y., 2018. Hydrodynamic mechanisms underlying periodic algal blooms in the tributary bay of a subtropical reservoir. *Ecol. Eng.* 120, 6–13.
- Yu, Y., Wang, P., Wang, C., Wang, X., 2018. Optimal reservoir operation using multi-objective evolutionary algorithms for potential estuarine eutrophication control. *J. Environ. Manag.* 233, 758–770.
- Zeng, H., Song, L., Yu, Z., Chen, H., 2006. Distribution of phytoplankton in the three-gorge reservoir during rainy and dry seasons. *Sci. Total Environ.* 367, 999–1009.
- Zhang, Y., Shan, L., Qian, X., Wang, Q., Qian, Y., Liu, J., 2011. Temporal and spatial variability of chlorophyll a concentration in Lake Taihu using MODIS time-series data. *Hydrobiologia* 661, 235–250.
- Zhang, Y., Yin, Y., Wang, M., Liu, X., 2012. Effect of phytoplankton community composition and cell size on absorption properties in eutrophic shallow lakes: field and experimental evidence. *Optic Express* 20, 11882–11898.
- Zhou, B., Shang, M., Wang, G., Feng, L., Shan, K., Liu, X., Wu, L., Zhang, X., 2017. Remote estimation of cyanobacterial blooms using the risky grade index (RGI) and coverage area index (CAI): a case study in the Three Gorges Reservoir, China. *Environ. Sci. Pollut. Res.* 24, 19044–19056.
- Zhou, B., Shang, M., Wang, G., Zhang, S., Feng, L., Liu, X., Wu, L., Shan, K., 2018. Distinguishing two phenotypes of blooms using the normalised difference peak-valley index (NDPI) and Cyano-Chlorophyta index (CCI). *Sci. Total Environ.* 628–629, 848–857.
- Zhu, K., Bi, Y., Hu, Z., 2013. Responses of phytoplankton functional groups to the hydrologic regime in the Daning River, a tributary of Three Gorges Reservoir, China. *Sci. Total Environ.* 450–451, 169–177.